Mössbauer Faraday Effect

R. M. HOUSLEY AND U. GONSER

Science Center, North American Rockwell Corporation, Thousand Oaks, California 91360

(Received 5 February 1968)

The dispersion associated with Mössbauer resonance absorption has been analyzed. Special attention is given to the problem of the rotation of linearly polarized recoil-free 14.4-keV γ rays transmitted through a resonantly absorbing material (transmitter) with longitudinal applied field (nuclear Faraday effect). A simple zero-velocity Mössbauer polarimeter and its operation are described. It has been used to measure the Faraday effect in the ferrimagnetic spinel $MgFe_2O_4$.

THE dispersion associated with Mössbauer resonance absorption has, with a relatively small number of exceptions,[1-7] been ignored up to the present. We discuss the magnitude of effects which result from this dispersion with special consideration of the Faraday effect. We derive an exact formula for the rotation expected with a simple Mössbauer polarimeter which has been previously described[5,6] and use this to analyze experimental data on the ferrite $MgFe_2O_4$.

The classical theory of electromagnetic radiation leads to a simple expression for the complex index of refraction ρ of a material containing N nonpolarized resonant absorbers of a single frequency per unit volume,[8]

$$\rho=1+\tfrac{1}{2}(\lambda\!\!\!^{-}Nf'\sigma_0)\left(\frac{x_0-x}{(x_0-x)^2+1}+i[(x_0-x)^2+1]^{-1}\right), \quad (1)$$

where we have introduced the normalized energy $x=2E/\Gamma$ and resonant energy $x_0=2E_0/\Gamma$; Γ is the linewidth. The quantity $f'\sigma_0$ is the total cross section per resonant absorber and $2\pi\lambda\!\!\!^{-}$ is the wavelength. Inserting values appropriate for Fe^{57}, we see that $\frac{1}{2}(\lambda\!\!\!^{-}Nf'\sigma_0)$ can be as large as 5×10^{-2}, for example, in stainless steel made with Fe^{57}.

Even for a single-line Mössbauer absorber, Eq. (1) must be modified to take account of the nonresonant electronic absorption in the absorber. Since this is a very weak function of energy compared to the nuclear resonance, we may take care of it by adding a constant α to the imaginary part of ρ.

$$\rho=1+\tfrac{1}{2}(\lambda\!\!\!^{-}Nf'\sigma_0)\left(\frac{x_0-x}{(x_0-x)^2+1}+i\{\alpha+[(x_0-x)^2+1]^{-1}\}\right), \quad (2)$$

where α is the total electronic cross section per unit volume divided by $Nf'\sigma_0$.

The phase change from that which would occur with no absorber present and the attenuation in amplitude of a wave traveling through a slab of material with ρ given by Eq. (2) are, respectively,

$$\varphi=\tfrac{1}{2}(nf'\sigma_0)[(x_0-x)/(x_0-x)^2+1] \quad (3)$$

and

$$A/A_0=\exp\left(-\tfrac{1}{2}(nf'\sigma_0)\{[(x_0-x)^2+1]^{-1}+\alpha\}\right), \quad (4)$$

where n is the number of resonance absorbers per unit area. The intensity is attenuated by Eq. (4) squared.

The maximum phase change for a given attenuation is obtained when $x_0-x=[(1+\alpha)/\alpha]^{1/2}$. For pure Fe^{57} at room temperature where $f'\approx0.8$, we have $\alpha\approx1/310$ and, correspondingly, $(x_0-x)_{\max}\approx17.6$. If the Fe^{57} is magnetized in a longitudinal (parallel to the γ-ray direction) magnetic field, the effective cross section of one of the outer lines for radiation of the appropriate circular polarization is $\frac{3}{8}(nf'\sigma_0)$. To illustrate the order of magnitude of phase shifts expected, consider an Fe^{57} foil of 10 mg/cm^2 thickness magnetized in a longitudinal field. At the appropriate distance outside one of the outer lines, γ rays of the correct circular polarization undergo a phase shift of ~2.1 rad, while the intensity is attenuated by the factor 0.38. γ rays of the opposite circular polarization undergo almost no phase shift and are only attenuated by the factor 0.62. Thus we are led to expect that under suitable conditions dispersion effects will be quite important in Mössbauer spectroscopy.

Generally, a Mössbauer absorber will have several resonant energies, and within each crystal grain or

[1] G. T. Trammell, Phys. Rev. **126**, 1045 (1962).
[2] P. Imbert, Phys. Letters **8**, 95 (1964).
[3] P. Imbert, J. Phys. (Paris) **27**, 429 (1966).
[4] S. Bernstein, E. C. Campbell, and C. W. Nestor, Jr., J. Phys. Chem. Solids **26**, 883 (1965).
[5] U. Gonser, *Hyperfine Structure and Nuclear Radiation*, edited by E. Matthias and D. A. Shirley (North-Holland Publishing Co., Amsterdam, to be published).
[6] U. Gonser and R. M. Housley, Phys. Letters **26A**, 157 (1968).
[7] M. Blume and O. C. Kistner, this issue, Phys. Rev. **171**, 417 (1968).
[8] W. K. H. Panofsky and M. Phillips, *Classical Electricity and Magnetism* (Addison-Wesley Publishing Co., Inc., Reading, Mass., 1962). Our Eq. (1) comes from their Eqs. (22)-(52) by relabeling the total cross section as $f'\sigma_0$ and by making the approximation valid for narrow lines that $\omega+\omega_0\to2\omega_0$. Also, since $n\approx1$, we have set $n=1+\frac{1}{2}(n^2-1)$.

magnetic domain of the absorber, these lines have definite polarizations. The general case, which is quite complicated, is discussed in Ref. 7. In the special case, where all of the lines have one or the other of two *orthogonal* partial or complete polarizations, we may define an index of refraction similar to Eq. (2) for each polarization.[9] If all resonant sites in the absorber are crystallographically equivalent, then these separate indices of refraction take the simple forms

$$\rho_1=1+\tfrac{1}{2}(\chi N f'\sigma_0)\sum_j a_{1j}^2\left(\frac{x_j-x}{(x_j-x)^2+1}+i\{[(x_j-x)^2+1]^{-1}+\alpha\}\right) \quad (5)$$

and

$$\rho_2=1+\tfrac{1}{2}(\chi N f'\sigma_0)\sum_j a_{2j}^2\left(\frac{x_j-x}{(x_j-x)^2+1}+i\{[(x_j-x)^2+1]^{-1}+\alpha\}\right). \quad (6)$$

The sums run over all the lines, and the factors a_{1j}^2 and a_{2j}^2 give the relative contributions of the different lines to each polarization. They satisfy the normalization condition

$$\sum_j a_{1j}^2=\sum_j a_{2j}^2=1, \quad (7)$$

and if no transitions overlap in energy they are proportional to the line intensities observed in the thin-absorber limit. If the projection of the angular momentum m along some axis is a good quantum number, a_{1j}^2 and a_{2j}^2 are products of the squares of the corresponding Clebsch-Gordan coefficients and the angular dependence factors for the individual nuclear transitions.[10]

All lines have one or the other of two orthogonal polarizations, and Eqs. (5) and (6) apply for any observation direction if all sites are equivalent and the spectrum contains only two lines, as is the case, for example, with a pure quadrupole interaction for Fe^{57}. These equations also apply for a pure magnetic hyperfine interaction if the observation direction is parallel or perpendicular to the quantization axis. These are, respectively, just the directions used to observe Faraday rotation[3,5,6] and magnetic double refraction[3,5] of the Mössbauer γ rays. In the case of a parallel field, the subscripts 1 and 2 stand for right and left circular polarization. In the transverse field they stand for linear polarization parallel and perpendicular to the field, respectively.

It is now simple to find the Faraday rotation of a linearly polarized γ ray of definite energy incident on a transmitter (absorber) which is longitudinally magnetized. We represent the incident γ ray as a superposition of right and left circularly polarized γ rays and let each proceed through the transmitter with the corresponding index of refraction. The attenuation in intensity of the two beams,

$$\exp\left[-nf'\sigma_0\left(\sum_j\frac{a_{1j}^2}{(x_j-x)^2+1}+\alpha\right)\right]\equiv\exp(-nf'\sigma_0\alpha)\exp[-t_1(x)] \quad (8)$$

and

$$\exp\left[-nf'\sigma_0\left(\sum_j\frac{a_{2j}^2}{(x_j-x)^2+1}+\alpha\right)\right]\equiv\exp(-nf'\sigma_0\alpha)\exp[-t_2(x)], \quad (9)$$

will generally be different. Recombining them with the appropriate phase shifts will yield emergent radiation with elliptical polarization. This may be resolved back into a linear component of relative intensity with respect to the incident beam of

$$\exp(-nf'\sigma_0\alpha)\exp[-t_m(x)], \quad (10)$$

where $t_m(x)$ is the greater of $t_1(x)$ and $t_2(x)$, and a circular component of relative intensity

$$\exp(-nf'\sigma_0\alpha)\,|\exp[-t_1(x)]-\exp[-t_2(x)]|. \quad (11)$$

The angle of Faraday rotation of the linear component δ is half the difference in phase shifts for the two polarizations:

$$\delta=\tfrac{1}{4}(nf'\sigma_0)\sum_j\frac{(a_{1j}^2-a_{2j}^2)(x_j-x)}{(x_j-x)^2+1}. \quad (12)$$

Since the electronic attenuation affects both circular polarizations equally, it does not change the Faraday rotation.

In our polarimeter, the longitudinally magnetized transmitter is placed between a Co^{57} in Fe metal source (polarizer) and an enriched Fe^{57} absorber (analyzer), both transversely magnetized by the fields H_S and H_A. The count rate $R(\omega)$ as a function of the angle ω between the two transverse fields is measured. Without the transmitter, we have

$$R(\omega)-R_B=R_{14}-fR_{14}A_0-\tfrac{1}{2}(fR_{14})A_1(1+\cos 2\omega), \quad (13)$$

where R_B is the background count rate and R_{14} is the total 14.4-keV count rate after electronic attenuation in the absorber is taken into account, as could, for example, be measured by moving the source rapidly

[9] We wish to thank Dr. M. Blume for discussions concerning this point.

[10] Even if m is not a good quantum number, the a_{1j}^2 and a_{2j}^2 coefficients may be computed in a straightforward manner. If nonequivalent sites are involved, f' may be different for the various sites and so cannot be factored out of the sums as in Eqs. (5) and (6). Even so, sometimes coefficients similar to a_{1j}^2 and a_{2j}^2 may be defined and indices of refraction similar to Eqs. (5) and (6) written. This will be discussed in a future publication.

with respect to the absorber, and f is the Debye-Waller factor of the source.

The factors A_0 and A_1 are

$$A_0=\int_{-\infty}^{\infty}\{I_1(x)\exp[-b_2(x)]+I_2(x)\exp[-b_1(x)]\}dx \tag{14}$$

and

$$A_1=\int_{-\infty}^{\infty}[I_1(x)-I_2(x)]\{\exp[-b_2(x)]-\exp[b_1(x)]\}dx, \tag{15}$$

where $I_1(x)$ and $I_2(x)$ are the source intensity functions (a sum of six Lorentzians for Fe metal) normalized so that

$$\int_{-\infty}^{\infty}[I_1(x)+I_2(x)]dx=1, \tag{16}$$

and $b_1(x)$ and $b_2(x)$ are the nuclear cross-section functions for the absorber, when $\omega=0$, defined similarly to the $t_i(x)$ functions. The subscripts 1 and 2 designate polarizations parallel and perpendicular to the fields H_S and H_A. The factor A_0 describes the isotropic attenuation of the 14.4-keV radiation due to overlapping or only partially polarized lines. In our case $A_0\approx 0$ and A_1 may to a good approximation be written as a sum of six integrals corresponding to the well-resolved emission and absorption lines. However, this treatment is general enough to apply to any case where matching polarized source and absorber are used. In particular, it will apply when the source and absorber lines are only partially polarized.

With the transmitter, the Faraday effect causes the different contributions to $R(\omega)-R_B$ to be rotated by different amounts $\delta(x)$ given by Eq. (12). The components may also be reduced in magnitude and partially converted to circular polarization by the nuclear attenuation in the transmitter, as described by Eqs. (10) and (11).

The counting rate $R(\omega)-R_B$ may be thought of as a sum of many contributions similar to Eq. (13), with R_{14} now standing for the 14.4-keV intensity after electronic attenuation in both transmitter and absorber is taken into account. This sum will again be a sinusoidal curve with the same period but will be shifted in phase and reduced in amplitude. Quantitatively, this may be written

$$R(\omega)-R_B=R_{14}-fRB_0-\tfrac{1}{2}(fR_{14})B_1\cos 2\omega-\tfrac{1}{2}(fR_{14})B_2\sin 2\omega, \tag{17}$$

where

$$B_0=\frac{1}{2}\int_{-\infty}^{\infty}[I_1(x)+I_2(x)]\,|\exp[-t_1(x)]-\exp[-t_2(x)]|\,\{\exp[-b_1(x)]+\exp[-b_2(x)]\}dx$$
$$+\frac{1}{2}\int_{-\infty}^{\infty}[I_1(x)-I_2(x)]\exp[-t_m(x)]\{\exp[-b_2(x)]-\exp[-b_1(x)]\}dx$$
$$+\int_{-\infty}^{\infty}\{I_1(x)\exp[-b_2(x)]+I_2(x)\exp[-b_1(x)]\}\exp[-t_m(x)]dx, \tag{18}$$

$$B_1=\int_{-\infty}^{\infty}[I_1(x)-I_2(x)]\exp[-t_m(x)]\{\exp[-b_2(x)]-\exp[-b_1(x)]\}\cos 2\delta(x)\,dx, \tag{19}$$

and

$$B_2=\int_{-\infty}^{\infty}[I_1(x)-I_2(x)]\exp[-t_m(x)]\{\exp[-b_2(x)]-\exp[-b_1(x)]\}\sin 2\delta(x)\,dx. \tag{20}$$

For the transmitter, the subscripts 1 and 2 stand for right and left circular polarization, whereas for the source and absorber they stand for linear polarizations. In cases where the polarizer lines are at least several natural widths from the transmitter resonance, $\exp[-t_i(x)]\approx 1$ and $\delta(x)\approx\delta(x_0)$, the value at the line center, over the whole region where the line has appreciable intensity. This gives the formula which we used previously.[6] The analysis for magnetic double refraction is very similar.

Magnesioferrite, $(Mg_zFe_{1-z})[Mg_{1-z}Fe_{1+z}]O_4$, is a partially inverse spinel with iron occupying tetrahedral (Fe) and more than half of the octahedral [Fe] sites. The quantity z is the fraction of Mg in the tetrahedral sites. The two sublattices are antiferromagnetically coupled. The ferrimagnetism is the result of an unbalanced Fe site occupation. The relative site occupation of the Fe ions, which determines the magnetization and net moment, can be varied with the annealing temperature and the cooling rate.[11] The sample in this experiment was quenched from 1400°C. The magnitude of the two internal magnetic fields at room temperature

[11] R. Pauthenet and L. Bochirol, J. Phys. Radium **12**, 249 (1951).

is nearly the same ($H_{(Fe)}$, $H_{[Fe]} \approx 500$ kOe). The spectra resulting from the two sublattices are unresolved. When an external field $\mathbf{H}_T$ is applied, the moments of the two sublattices are magnetized parallel [Fe] and antiparallel (Fe) to the applied field. This fact is indicated in Fig. 1 by the splitting of the Mössbauer lines, especially the outer lines. The spectrum in Fig. 1 was taken with a $MgFe_2O_4$ absorber (2.8 mg/cm², 67.4% enriched in Fe^{57}) in a longitudinal magnetic field ($\mathbf{H}_T = 55$ kOe) and a single-line Co^{57}–Cu source both at room temperature. Note that the effective field at the nuclei is in opposite direction to the atomic moment; thus a decrease in splitting is expected for the [Fe] sublattice magnetized parallel to $\mathbf{H}_T$ and an increase in splitting for the (Fe) sublattice. Having $\mathbf{H}_T$ along the γ-ray propagation direction, the $\Delta m = 0$ lines vanish.

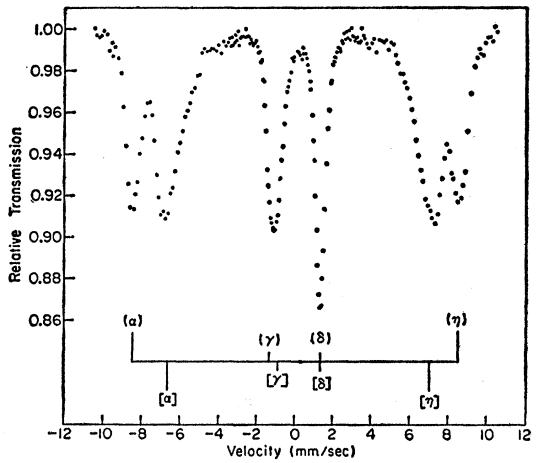

FIG. 1. Transmission spectra from a polycrystalline $MgFe_2O_4$ sample (2.8 mg/cm², 67.4% enriched in Fe^{57}) in a longitudinal magnetic field ($\mathbf{H}_T = 55$ kOe) taken with a Co^{57}–Cu source. Source and absorber were at room temperature. The line positions of the tetrahedral (Fe) and octahedral [Fe] sublattices are indicated.

In Fig. 2 the room-temperature Mössbauer spectrum of a $MgFe_2O_4$ sample (37.0 mg/cm², 67.4% enriched in Fe^{57}) taken with a single-line Co^{57}–Cu source is shown. An external field of 55 kOe was applied parallel to the propagation direction of the γ rays. In Fig. 2 the spectrum was shifted by 0.23 mm/sec towards positive velocity to make zero velocity correspond to a Co^{57}-α-Fe source. The stick diagram under the spectrum indicates the positions of the hyperfine spectra of the two Fe sublattices. These positions were determined from the spectrum in Fig. 1 outer lines. The line positions and intensities from the Co^{57}-α-Fe source and the α-Fe absorber are indicated at the top and the bottom of Fig. 2, respectively.

The relative transmission as a function of the angle ω between source and absorber magnetic fields is shown in Fig. 3. The pattern has been shifted by 19° (see arrow). When $\mathbf{H}_T$ has its north pole oriented toward the absorber and one is looking along the propagation direction of the γ rays, a clockwise rotation of the plane of polarization is observed. By reversing the magnetic field applied to the transmitter, the Faraday effect was observed in opposite direction.

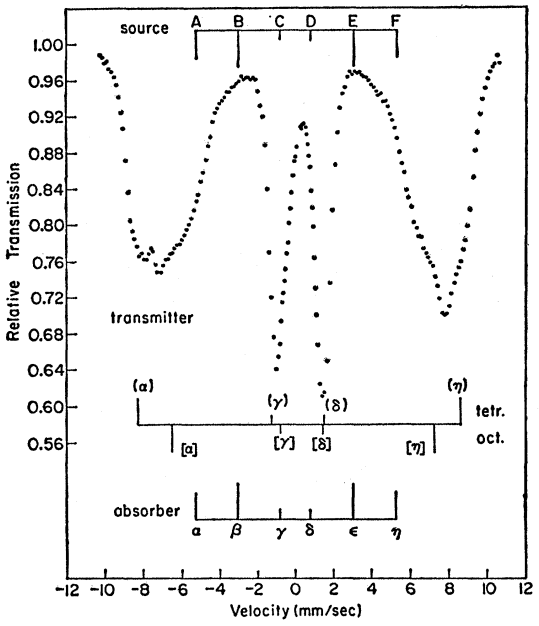

FIG. 2. Transmission spectra from a polycrystalline $MgFe_2O_4$ sample (37.0 mg/cm², 67.4% enriched in Fe^{57}) in a longitudinal magnetic field ($\mathbf{H}_T = 55$ kOe) taken with a Co^{57}–Cu source. Source and absorber were at room temperature. The spectrum is shifted by 0.23 mm/sec towards positive velocity (isomer shift versus α-Fe). The positions of the tetrahedral (Fe) and octahedral [Fe] sublattices are indicated. At the top and the bottom the six Zeeman lines from a Co^{57}-α-Fe source and α-Fe absorber, respectively, with their respective intensities, are shown.

The highly Fe^{57}-enriched $MgFe_2O_4$ sample has the following effects: It absorbs to a great extent the *C* and *D* lines of the source. Most of one circular polarization from the *A* and *F* lines is absorbed while the other circular polarization is transmitted but does not contribute to the Faraday rotation. In evaluation of the expected rotational shift, the small contributions from

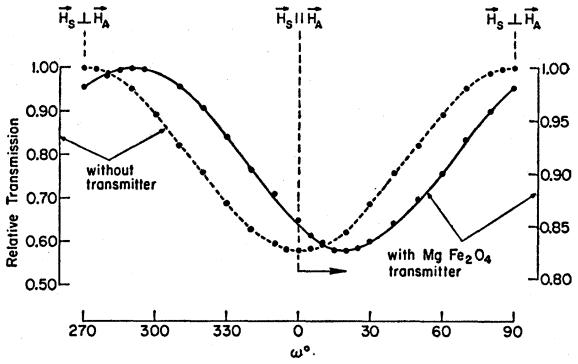

FIG. 3. Relative transmission of a Co^{57}-α-Fe source (polarizer $\mathbf{H}_S$) and an α-Fe absorber (analyzer $\mathbf{H}_A$) in transverse magnetic fields without and with $MgFe_2O_4$ transmitter (37.0 mg/cm², 67.4% enriched in Fe^{57}) in a longitudinal magnetic field ($\mathbf{H}_T = 55$ kOe) as a function of angle ω between $\mathbf{H}_S$ and $\mathbf{H}_A$.

the A, C, D, and F lines are neglected. The strongest B and E lines are largely transmitted and are both Faraday rotated in the same direction.

The rotation δ_E for the E line from the source can be represented by a sum of contributions from the octahedral and tetrahedral sites,

$$\delta_E=\delta_{[E]}+\delta_{(E)}.$$

The fraction of Mg in tetrahedral sites is z; thus $\frac{1}{2}[1+z]$ and $\frac{1}{2}(1-z)$ are the fractions of Fe in the octahedral and tetrahedral sites, respectively. Therefore,

$$\delta_{[E]}=\tfrac{1}{4}(nf'\sigma_0)\tfrac{1}{2}(1+z)\sum_j \frac{a_{[j]}^2(x_E-x_{[j]})}{(x_E-x_{[j]})^2+1}$$

and

$$\delta_{(E)}=-\tfrac{1}{4}(nf'\sigma_0)\tfrac{1}{2}(1-z)\sum_j \frac{a_{(j)}^2(x_E-x_{(j)})}{(x_E-x_{(j)})^2+1}. \quad (21)$$

Similar equations can be written for the B source line. The line positions on the positive and negative velocity side in regard to the E and B lines are very similar; thus the rotation experienced by the E and B lines is approximately the same. This can be seen by inserting the values for the B line into Eqs. (21). The observed rotation of the E and B lines in this experiment was 19° or $\approx$0.33 rad. Solving Eqs. (21) for z, the fraction of Mg in tetrahedral sites, assuming a recoil-free fraction of $f'=0.7$ for both sites, a value $z=0.26$ is obtained. This value agrees with measurements obtained by other techniques[11] for a $(Mg_z, Fe_{1-z})[Mg_{1-z}, Fe_{1+z}]O_4$ sample quenched from 1400°C.

Discussions with Dr. R. W. Grant, Dr. A. H. Muir, Jr., and Dr. H. Wiedersich are appreciated. We thank J. W. Savage for preparing the Fe^{57} enriched $MgFe_2O_4$ sample and M. R. Bloombaum and K. Rasmussen for technical assistance.

PHYSICAL REVIEW VOLUME 171, NUMBER 2 10 JULY 1968

Non-Closed-Shell Linear Chain: The H_{4n} System

W. T. Kwo

Chemical Physics Research Laboratory, The Dow Chemical Company, Midland, Michigan

(Received 14 March 1968)

The low-lying energy levels of a non-closed-shell linear chain consisting of $4n$ hydrogen atoms, each occupying a vertex of a regular polygon of $4n$ sides and contributing a single $1s$ electron, are studied with electron correlation taken into consideration in an approximate way within the framework of Löwdin's extension of the Hartree-Fock method. The nature of the wave functions and energy expressions for such a system with both orbital and spin degeneracies is discussed. It is shown that in the $n=3$ case the energy levels have the correct asymptotic behavior as the interatomic separation R assumes large values, and that a change of lattice spacing in the limit of small R could lead to a magnetic transition.

I. INTRODUCTION

In this paper, we consider the low-lying energy levels of a non-closed-shell linear chain, with both orbital and spin degeneracies, consisting of $4n$ hydrogen atoms each occupying a vertex of a regular polygon of $4n$ sides and contributing a single $1s$ electron. We account for electron correlation effects in an approximate way within the framework of Löwdin's extension of the Hartree-Fock method[1] through the use of wave functions of the form

$$\Psi={}^{(2S+1)}OO_R\Phi. \quad (1)$$

Here ${}^{(2S+1)}O$ is a spin projection operator[2] for selecting a pure spin state of multiplicity $(2S+1)$, O_R is an operator that acts upon the spatial coordinates of the electrons and leads to a wave function belonging to an irreducible representation of the group of the spin-free Hamiltonian H,[3] and Φ represents a linear combination of antisymmetrized products of one-electron wave functions $\psi_{j\mathrm{I}}$ and $\psi_{j\mathrm{II}}$ of alternant character.[4,5] Expressions for the expectation values of the Hamiltonian H for the low-lying energy levels are then determined by evaluating

$$E=\langle\Psi\mid H\mid\Psi\rangle/\langle\Psi\mid\Psi\rangle. \quad (2)$$

We present the results of calculations for the $n=3$ case carried out at interatomic distances varying from large separations to values smaller than the equilibrium distance, and show that a magnetic transition occurs when the interatomic distance R is changed in the limit of small R.

II. WAVE FUNCTIONS AND ENERGY EXPRESSIONS

Let us first define X_0 as the identity operator, Y_0 as a spatial reflection operator,[6] P as representing a

[1] P.-O.Löwdin, Phys. Rev. **97**, 1509 (1955).
[2] P.-O. Löwdin, Advan. Phys. **5**, 1 (1956).
[3] P.-O. Löwdin, Phys. Rev. **97**, 1474 (1955).
[4] W. T. Kwo, Phys. Rev. Letters **12**, 563 (1964).
[5] W. T. Kwo, Phys. Letters **16**, 115 (1965).
[6] J. C. Slater, *Quantum Theory of Molecules and Solids* (McGraw-Hill Book Co., New York, 1963), Vol. 1, Chap. 8.